Engineered Science
DOI: https://dx.doi.org/10.30919/es1878

Application of Fire Extinguishing Agent from Cellulose Ether to Extinguish Forest Fires Using a Water Bottle Rocket

Nuttabodee Viriyawattana* and Surachat Sinworn*

Abstract

Water hyacinth, an invasive aquatic weed disrupting ecosystems, reproduces rapidly and causes a significant environmental challenge due to its difficulty in eradication. Thus, the utilization of this plant for fire suppression not only helps mitigate environmental concerns, but also enhances its economic value. This process involves synthesizing a water hyacinth to methyl cellulose, a type of cellulose ether. The synthesized compound is further processed into a hydrogel. When this hydrogel exposes to heat, it forms a protective coating over combustible materials, therefore, a temperature reduced and an oxygen for combustion limited. This prominent essence enhances its performance in wildfire suppression. This hydrogel contains fire extinguishing agents which is better adhesive to combustible wood surfaces than the conventional fire extinguishing substances. Thereby, the effectiveness in wildfire suppression is multiplied. When applied this hydrogel in water-propelled rockets deploying from a safe distance, the risk to firefighter on fire control duty is significantly reduced. The experimental trials were conducted using a water-propelled rocket at a pressure of 4 bar with various water levels in the container (k_o) at four different levels of 20%, 25%, 33%, and 50%. The results indicated that at 20% water level, the rocket achieved the highest velocity and the longest travel distance compared to the others. In the test for fire suppression performance on a Class 2A fire at 20 meter distance, the combination of MAP (Mono Ammonium Phosphate) and Methyl Cellulose demonstrated a superior fire-extinguishing efficiency was compared to using MAP alone. This combined formulation effectively reduced the radiant heat emission to 35°C, using 7 seconds to extinguish fire. Also, it formed a protective coating over the fuel surface to preventing from re-ignition after suppression.

Keywords: Fire extinguishing agent; Cellulose ether; Forest fire; Bottle rocket.
Received: 24 April 2025; Revised: 30 October 2025; Accepted: 10 November 2025
Article type: Research article.

1. Introduction

A wildfire normally occurs in vegetation-rich rural areas depending on the type of plants represented. A wildfire can be specifically categorized into various types, including peatland fire, forest wildfire, desert wildfire, grassland wildfire, hill wildfire, peat wildfire, vegetation wildfire, and savanna wildfire. A wildfire can also be classified based on the ignition causes, the physical characteristics, the combustible materials, and the consequence of weather conditions. A wildfire endangers not only for the property, but also the casualty of human lost when the fire spreads to populated areas. A smoke from wildfire causes the health effect on individuals.[1-3] A wildfire is a serious global environmental threat due to its rapid speed and uncontrollable spread. It causes an impactful threat to ecosystem, human, and property. Therefore, a wildfire becomes a major obstacle to economic development.[4-6] Traditional fire suppression agents, such as water, dry chemical powder, and foam, exhibit the varied degrees of fire-extinguishing performance, however, they are subject to limitations in terms of efficiency, environmental impact, and resource utilization. For instance, water although widely available and easily transportable, is highly vulnerable at high temperature, so it is unable to penetrate into high-temperature zones within flame. Thus, a large amount of water is demanded, leading to a low economic performance,[7] and a high risk of fire recurred. Similarly, the dry chemical powder and foam are unable to penetrate deeply into burning flames, resulting in inadequate coverage of fire-affected areas. Additionally, these agents leave behind residues which are difficult to clean up.[8,9] In contrast to the traditional fire suppression materials, a hydrogel exhibits the advantageous properties such as water retention, adhesion, and cooling

Occupational Health and Safety Program, Faculty of Science and Technology, Suan Dusit University, 288/1-3 Sirinthon Avenue, Bangkok, 10700, Thailand
*Email: nutta_v@hotmail.com (Nuttabodee Viriyawattana), surachat5601@gmail.com (Surachat Sinworn)

capability.[10] These properties facilitate a fire suppression by providing partial coating, and reducing water consumption. Therefore, it enhances a fire-extinguishing performance, a combustion inhibition, and an ability to reduce temperature across various materials including coal and mining.[11-13] However, a hydrogel commonly exhibits a low fluidity which reduces the ability to fire penetration and spray delivery. This results in a limitation of area coverage, and a difficulty in residue cleaned up. In the result of materials science advancement, the recent exploration of new fire suppression materials has consistently gained more attention.[14] The temperature-responsive hydrogels with the reversible sol-gel phase transition by temperature fluctuations, gives a promising solution to manage a wildfire. These smart polymeric materials transfer into a sol (liquid state) at temperatures below their critical solution temperature (CST). The liquid form facilitates an ease of storage and transportation, and a performance of penetration. Conversely, at an exceeding threshold temperature, they transform into gels, adhering to surfaces.[15] This phase transition effectively inhibits an oxygen supply, and reduces a smoke emission, thereby they overcome the limitations of traditional fire suppression methods.

Wildfire suppression strategies can be categorized into two primary approaches:[16]

1) Proactive Wildfire Suppression: The proactive wildfire suppression involves the direct attack methods by firefighters, fire trucks, and/or aerial firefighting aircraft to combat the fire at its active edge. The most effective approach is attacking the Fireline against the wind direction. However, due to an unpredictable spread of wildfire, this method may place a significant safety risk, and it is not always preferrable. So, this approach is only suitable for low-intensity flames, as miscalculations in fire spread speed and flame length can endanger individuals. Additionally, an increase of wind speed and a challenging terrain may further complicate operations, increasing the likelihood of firefighters surrounded by flames.

2) Defensive Wildfire Suppression: When the proactive wildfire suppression is not possible due to excessively high flames or terrain contamination (e.g., unexploded ordnance), the defensive wildfire suppression shall be deployed. This involves a firebreak or utilizing any existence of fire-resistant barriers *e.g.* roads or walkways to halt fire progression. It is crucial to continuously monitor surrounding areas, and immediately extinguish secondary fires caused by embers or firebrands to prevent from a wildfire inattention. The challenges of wildfire suppression have led to the new development of firefighting techniques [17] to aim for: 2.1) Enhancing a firefighter safety; Particularly, the deployment of a continuous water cannons, which project water ahead of advancing firefighters, acts as a protective barrier between them and the wildfire. 2.2) Saving an extreme fire entrapment; In some cases, firefighters trapped in a rapidly spreading fire, making escape impossible. Although they may attempt to seek shelter under fire tents, these protective gears often inadequate, leading to fatalities.[18,19] A 35-kilogram unmanned aerial fire suppression device has been developed which is housed within an aluminum alloy casing. The fire-extinguishing agent used in this system is a commercial dry chemical powder. The device has the ignition mechanism as a military-standard fuse. Upon detonation near the ground (approximately 3 meters), the fire extinguishing agent will be released. However, this product exhibits several limitations, including a small loading capacity, a complex height adjustment for detonation after fuse activation, and an adhesion tendency for the extinguishing agent into a chunk upon explosion. As a result, the device proves ineffective in controlling an elevated fire, such as a fire at rooftop during wildfire spread.[20] The purpose of this research aimed to develop a fire suppression system using a water-propelled rocket equipped with a fire-extinguishing agent which formed into a gel coating on the surface of combustible materials. It was designed to enhance the safety and efficiency of ground-based firefighters in combating wildfires. There were various water-propelled aerial systems, such as personal jetpacks.[21,22]

Those demonstrated an agility and flight capability. However, these systems remained a manual or a semi-automated system. In order to get a fully automated operation, the control mechanism must be able to manage both water flow and nozzle positioning. Additionally, motion control methods must be relatively straightforward, including Proportional-Derivative (PD) control,[23] Proportional-Integral-Derivative (PID) control,[24] and Proportional control plus velocity feedback.[25] To enhance these capabilities for automated fire suppression, using water sources as a propelling mechanism for aerial systems offered a practical solution. This approach involved launching a water-propelled rocket into the Fireline. It detonated upon exposure to extreme heat, dispersing fire-extinguishing substances across the affected area. This mechanism provided a temporary fire suppression, allowing firefighters an additional time to establish firebreaks and to prevent from the flame encirclement, which could endanger firefighters. This new research was intentional to address the existing limitations of conventional fire suppression methods.[26] The fire-extinguishing chemical was deployed upon blast dispersion and the interaction between shock waves and fire. There were extensive researches conducted on blast dispersion mechanisms, while the research on the interaction between shock wave had been conducted on the interaction between shock wave and wild fire,[27] as well as the research of flame instabilities induced by shock wave and flame interactions.[28,29] Additionally, there were various researches on rocket-based fire suppression techniques for a long-range firefighting application,[30] demonstrating a promising potential for the adaptation in wildfire fighting strategies.

2. Materials and methods

2.1 Factors of propulsion stability of water-propelled rockets

The deployment of water-propelled rocket involved a linear motion along with an angled trajectory, allowing for direct propulsion in a predetermined direction. The Evaluation of the stability of water-propelled rocket considered a linear motion within the vertical plane, while neglecting rotational dynamics, in the regard of the similar principle to an aircraft flight stability analysis (Fig. 1). Key considerations included an impact of wind forces on the rocket, which may cause deviations from the vertical trajectory. For the stable rocket, it must generate a restorative moment which could redirected the rocket back to its original vertical alignment.

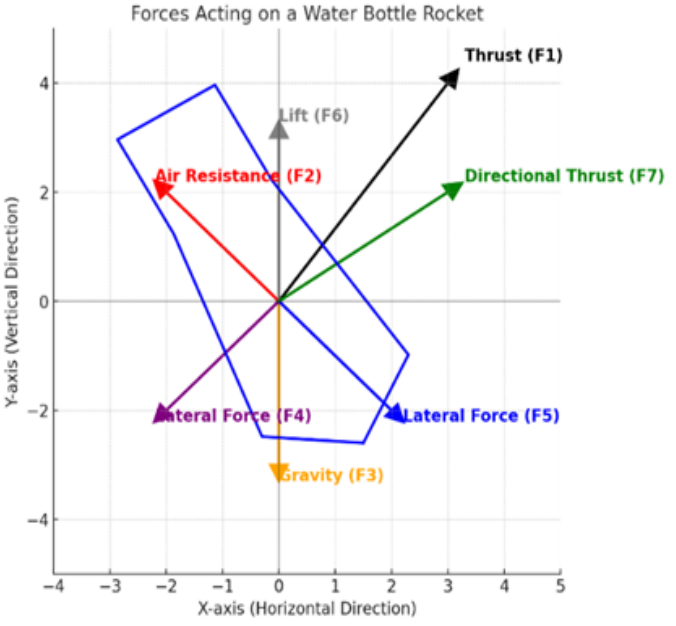

Fig. 1: Direction of driving force and other forces.

Note: F_1: Thrust force, F_2: Air resistance (drag), F_3: Gravitational force, F_4: Gravitational force in thrust's direction, F_5: Gravitational force in thrust's perpendicular direction, F_6: Difference between thrust force and counteracting forces, F_7: Total resultant force.

The stability of water-powered rockets was influenced by wind forces that may cause deviation from the intended vertical path. Stability was achieved when the center of mass was positioned higher than the aerodynamic center of the fins, ensuring the rocket returns to its vertical trajectory after any deviation.

As the rocket moved with an initial velocity U_0, it directed as the angle α of trajectory. The fins generated both the lifting force (Lf) and the dragging force (Df), acting at the aerodynamic center of the fins. The fins were constructed from paper sheets and were designed as symmetry Airfoil, with their aerodynamic center located at ¼ of the chord length. The center of gravity of the fins (CGfin) was positioned at the geometric center of the fin plate. Therefore, if α was small, the moment around the rocket's center of gravity (CG) could be expressed as:[31]

$$M = \left[L_f \cos\alpha + D_f \sin\alpha\right]\left[l_{CG} - \left(l_f + \frac{1}{4}C_f\right)\right] \quad (1)$$

$$M \cong L_f\left[l_{CG} - \left(l_f + \frac{1}{4}C_f\right)\right] \quad (2)$$

when

L_{CG} = The distance from the tip of the bottle to the center of gravity of the rocket.

L_f = The distance from the tip of the bottle to the center of gravity of the fins.

C_f = The cord length of the fins

Considering Eq. (1), the water-propelled rocket exhibited a flight stability as defined in the initial criteria when the position of the center of gravity (CG) satisfied the condition outlined in Eq. (2). This implied that the position of rocket's center of gravity must be above the position of the fins' aerodynamic center of gravity.

2.2 Rocket Motion Equations

The motion of water-propelled rockets was governed by the following Eqs. (3-5):[32]

$$m\frac{dv}{dt} = F - k(v)^2 - mg\sin(\theta) \quad (3)$$

$$v\frac{d\theta}{dt} = -g\cos(\theta), \frac{dm}{dt} = -\beta \quad (4)$$

$$\frac{dx}{dt} = v\cos(\theta), \frac{dy}{dt} = v\sin(\theta) \quad (5)$$

where m: was the rocket's mass (including water), θ: was the flight angle, F: was the thrust, v: was the rocket's velocity, R: was air resistance, β: was the water flow rate, and g: was gravitational acceleration.

2.3 Thrust generated by water ejection

A water-propelled rocket differed from any conventional fuel-based rockets, as its thrust was generated by the ejection of water, and the subsequent air propulsion that occurred after the water was released. This thrust arose from the acceleration of water due to pressure differences, where the initial pressure P_0 inside the bottle exceeded the ambient atmospheric pressure P_a (Fig. 2). First, considered the thrust generated by water ejection. When water (density: ρ) was expelled through a nozzle with cross-sectional area A at a velocity u, the mass dm of water ejected within an infinitesimal time interval dt could be described by the following equation:[32]

The flight of a water bottle rocket is a fascinating demonstration of fundamental physics, driven by the dynamic interaction of various forces. Propulsion (F1), generated by the jet of water, initiates and maintains upward motion, battling gravity (F3), which continually pulls it down. As the rocket accelerates, air resistance (F2) increasingly resists its motion, dictating its flight path and limiting its maximum efficiency. Meanwhile, aerodynamic lift (F6) and lateral forces (F4, F5),

are largely managed through design features such as fins and careful alignment of the center of mass relative to the center of pressure, help stabilize the rocket, prevent uncontrolled rollovers, and maintain a predictable trajectory. Even more advanced concepts, such as directional propulsion (F7), while not applicable in a typical water bottle rocket, demonstrate the broader principles of attitude control required for increasingly complex spacecraft. From powerful initial thrust to soft landings, each stage of a water bottle rocket's flight is a testament to Newton's laws of motion and the principles of aerodynamics. This simple yet effective model provides invaluable insight into the complex engineering challenges faced in real-world rocketry, offering a tangible and engaging way to explore the forces that allow us to conquer the skies and beyond. The ability to manipulate variables such as pressure, water volume, and rocket shape to improve performance directly reflects the iterative design process in aerospace engineering, making the bottle rocket a prime example of physics in action. The ability to manipulate variables such as pressure, water volume, and rocket shape to improve performance directly reflects the iterative design process in aerospace engineering, making the bottle rocket a prime example of physics in action. The ability to manipulate variables such as pressure, water volume, and rocket shape to improve performance directly reflects the iterative design process in aerospace engineering, making the bottle rocket a prime example of physics in action.

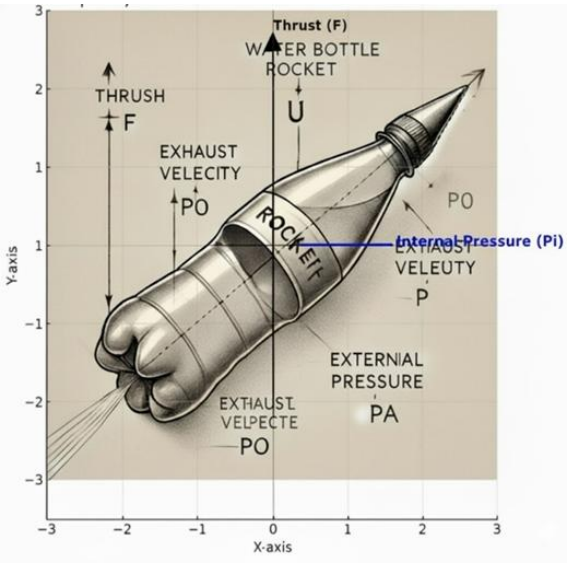

Fig. 2: Thrust Model.

Note: F: Thrust force, P_0: Internal pressure of the bottle, P_a: Atmospheric pressure, A_0: Cross-sectional area of the tank, u_0: Flow velocity within the tank, A: Cross-sectional area of the injection port, u: Flow velocity at the injection port.

$$dm = \rho A u.\, dt \tag{6}$$

The impulse force F·dt exerted on the rocket could be calculated by considering the ejection of mass (dm) in the opposite direction at velocity u:

$$F.\, dt = dm.\, u \tag{7}$$

By substituting Eq. (7) and (8) into this equation and rearranging the terms, the thrust force (F) of the rocket could be derived as follows:

$$F = \rho A u^2 \tag{8}$$

Assuming that the cross-sectional area of the tank was A_0, the flow velocity within the tank was u_0, the cross-sectional area at the injection port was A, and the flow velocity at the injection port was u. The following equations were derived from Bernoulli's equation and the continuity equation, which were the fundamental principles of fluid mechanics.

$$\frac{1}{2}\rho u^2 + P_a = \frac{1}{2}\rho u_0^2 + \rho g h + P_0 \tag{9}$$

$$u.\, A = u_0.\, A_0 \tag{10}$$

where P_a represented the atmospheric pressure, P_0 represented the internal pressure of the tank, g was the gravitational acceleration, and h was the height from the injection port to the water surface inside the tank. From Eq. (9) and (10), the following equation could be derived as:

$$u = \frac{1}{\sqrt{1-\left(\frac{A}{A_0}\right)^2}}\sqrt{\frac{2(P_0-P_a)}{\rho} + 2gh} \tag{11}$$

By substituting u from Eq. (11) and (12) into the thrust equation (F), the thrust generated by water ejection could be expressed as follows:

$$F = \frac{2A}{1-\left(\frac{A}{A_0}\right)^2}(P_0 - P_a + \rho g h) \tag{12}$$

The pressure (P_0) inside the tank decreased rapidly during water ejection; however, this change could be considered as the adiabatic process.

2.4 Thrust generated by air ejection

Compressed air still remained inside the tank after water ejection completed. When the remaining compressed air kept releasing, the rocket still gained the additional thrust, and continued to accelerate. In this analysis, the pressure (P_0) and density (ρ_0) of the air inside the tank were considered. The air exited the tank at the atmospheric pressure (P_a). At the injection port, there were the values of the gas as the air pressure (P_1) and density (ρ_1). The exit velocity (u_1) could be determined using the compressible fluid flow Eq. (13-20).[32]

$$u_1 = \sqrt{\frac{2\gamma}{\gamma-1}\cdot\frac{P_0}{\rho_0}\left\{1-\left(\frac{P_1}{\rho_0}\right)^{\frac{\gamma-1}{\gamma}}\right\}} \tag{13}$$

where γ represented the heat capacity ratio of air, and if γ = 1.4, substituting and rearranging the terms, the exit velocity (u_1) could be determined using the following equation:

$$u_1 = \sqrt{7 \cdot \frac{P_0}{\rho_0}\left\{1 - \left(\frac{P_1}{P_0}\right)^{\frac{2}{7}}\right\}} \quad (14)$$

Pressure (P_1) at the injection port was not always equal to the external pressure (Pa)

When the exit velocity (u_1) of the ejected gas did not exceed the speed of sound, the injection port pressure (P_1) ws assumed to be approximately equal to the external pressure (P_a). However, due to the significant pressure difference between the interior and exterior of the tank, the flow velocity could not exceed the speed of sound, the velocity even increased, the injection port pressure (P_1) did not decrease to meet the external pressure (P_a).

$$P_1 = \left(\frac{2}{\gamma+1}\right)^{\frac{\gamma}{\gamma-1}} \cdot P_0 = 0.528P_0 > P_a \quad (15)$$

This condition was referred to as choking (the flow blockage). The thrust force (F_a), which was the reaction to the momentum transferred to the expelled air, was given by $\rho_1 A u_1^2$, similar to the case of water ejection. The following equation was derived using the adiabatic expansion equation.

$$F_a = \rho_1 A u_1^2 = 7AP_1\left\{\left(\frac{P_0}{P_1}\right)^{\frac{2}{7}} - 1\right\} \quad (16)$$

When the injection port pressure was higher than the atmospheric pressure, an additional thrust force (F_p), known as the pressure thrust, arose due to the pressure difference. This additional thrust was expressed in the following equation.

$$F_p = A(P_1 - P_a) \quad (17)$$

The total thrust force - F, of the water propelled rocket could be determined from the following equation:

$$F = F_a + F_p = 7AP_1\left\{\left(\frac{P_0}{P_1}\right)^{\frac{2}{7}} - 1\right\} + A(P_1 - P_a) \quad (18)$$

Where the following conditional expression could be replaced by Pr

$$0.528 \times P_0 \geq P_a \rightarrow P_1 = 0.528 \times P_0 \quad (19)$$

$$0.528 \times P_0 < P_0 < P_a \rightarrow P_1 = P_a \quad (20)$$

Thrust (F) is the force that propels the rocket upwards. In a water bottle rocket, this thrust is caused by the water and compressed air being expelled from the nozzle of the bottle at high speed according to Newton's third law. This action of forcing the masses (water and air) downwards creates an equal and opposite reaction force, which is the thrust that pushes the rocket upwards. The exhaust velocity (U) is the speed at which the water and air are expelled from the nozzle of the rocket. In the figure, the downward pointing 'U' arrow represents the direction and velocity of the exhaust gases being expelled. The greater the velocity and mass of water expelled, the greater the thrust exerted on the rocket. The internal pressure (Pa) is the pressure of the compressed air inside the bottle. To prepare a water bottle rocket, air is pumped into the bottle partially filled with water to create high internal pressure. This high internal pressure is the primary driving force that pushes the water out of the nozzle, creating thrust. Increasing the pressure inside the bottle creates more thrust. The external pressure (P) is the pressure around the rocket, with the rocket's thrust being influenced by the difference between the internal pressure at the nozzle and the external pressure. When the internal pressure is reduced to equal to the external pressure, the propulsion force due to the pressure stops. In summary, Fig. 2 shows that a water bottle rocket's upward flight is achieved by converting the potential energy of the compressed air into the kinetic energy of the expelled water, which creates the thrust needed to overcome gravity and air drag, propelling the rocket upwards into the air.

2.5 Design of the water propelled rocket

The design considered the flight stability of a water propelled rocket made by plastic bottle (Fig. S1). It was a 700 ml carbonated beverage bottle. The rocket fins were made from paper sheets in rectangular form. The details of this rocket were captured as follows:

Mass of the rocket body excluding fins and water: $m_{body} = 0.07\ kg.$,The entire rocket length from a reference line to the nose tip: 0.34 m., The rocket diameter: D = 0.06 m., The height of the rocket's center of gravity: $l_{body} = 0.18$ m.,The initial water level in the rocket: $2l_w = 0.15$ m., The density of the paper sheet for rocket fins: $\rho_f = 0.46\ \mathrm{kg/m^2}$., The number of fins: $n_f = 4$., The fin chord length: $C_f = 25\%\ of\ l_{body}$, The fin width b_f 25% of l_{body}., The fin position l_f 20% l_{body}.

2.6 The optimal water pressure for rocket launch

The assumption was that the water ejection from the rocket occured instantaneously. Under this hypothesis, the reduction in velocity due to the gravitational potential energy of the bottle and water during the ejection process with a height increase, as well as changes in ejection velocity, did not need to be considered. Additionally, it was assumed that the rocket's surface was smooth, and the surface friction could be negligible from an air resistance. It was also considered that the air and water compression was neglected when the water was treated as an incompressible fluid. By these experiment conditions, the simulated entity was modeled in a 2-liter plastic bottle. Water was injected into the bottle, followed by the compressed air to increase its pressure. The initial compressed pressure varied at P_0 = 4 bar, with the various initial water ratios (k_0) set of 0.20, 0.25, 0.33, 0.50, and 0.70 respectively.[32] The rocket was mounted on a launch pad as illustrated in Fig. S2.

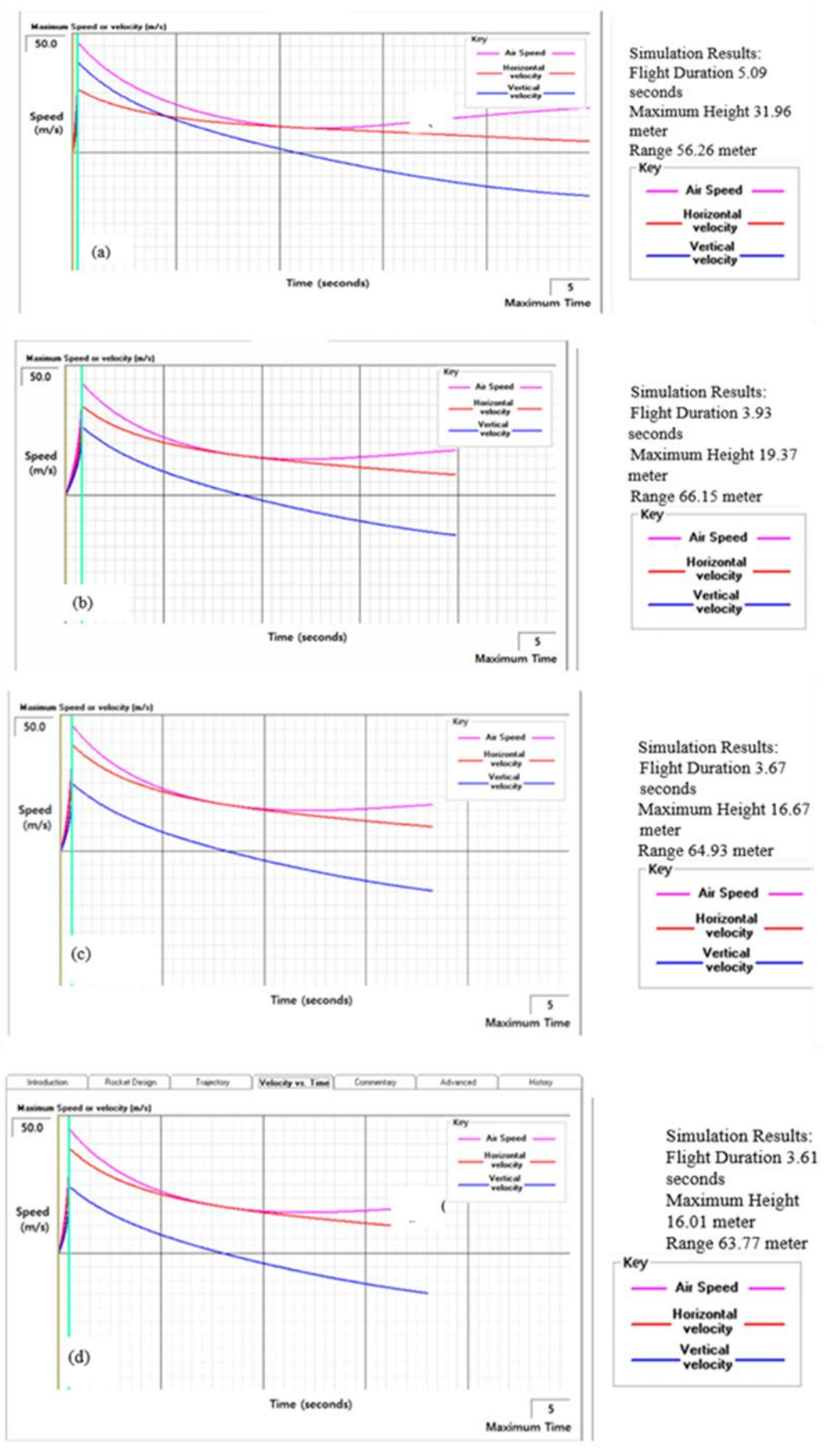

Fig. 3: Initial water retaining volume in the bottle was 20% (a), 25% (b), 33% (c) and 50% (d) at a pressure of 4 bar.

2.7 Fire extinguishing pack

A fire extinguishing pack was installed at the nose cone of the water propelled rocket. Each pack was weighed at 400 grams contained Mono Ammonium Phosphate (MAP) at 80% (320 g.), Nano-cellulose ether (Methyl Cellulose; MC) at 19% (76 g.), and the additive to replace water reaction at 1% (4 g.). This compound Pack was illustrated in Fig. S3. The ignition compound was made by Aluminum powder at 0.5 g, Potassium chlorate powder at 0.5 g. This extinguishing pack could cover an average 5 - 8 square meters of fire area.

2.8 The test to destination target using simulation software

The test of direction and range of the rocket were done by Water Rocket Simulation ver. 1.2 program to see the trajectory and the falling distance. After that, they were subsequently validated through the field testing, 12 times repeatedly evaluating the accuracy of the water propelled rockets.

2.9 The study on fire suppression performance of dry chemical powder agents containing nano-cellulose ether on class a fire

The study aimed to evaluate the fire suppression performance of dry chemical powder agents containing nano-cellulose ether on Class A fire with 4A rating. For the test, 120 wooden pallet samples were prepared, each with a cross-sectional dimension and length of 45 × 45 × 850 mm. These were stacked into 15 layers with 8 pieces per layer, and tested in an open-air environment. The wooden samples were stacked on a metal platform with the dimension of 1,000 × 1,000 × 400 mm. The pile of wooded pallet was arranged in a rectangular form and secured with nails around the outer layers. A steel tray with the dimension of 1,525 × 1,525 × 100 mm was placed beneath the metal platform and woodpile, following the ANSI/UL 711 (2007) standard. This arrangement was to test a fire suppression capacity equivalent to 4A rating. Gasohol E20 fuel was filled to the tray with the volume of 2.0 cubic decimeters. The fuel was ignited. Allow the fire to burn and spread to the top 2-3 layers of the woodpile for 5 to 10 minutes, or until the fuel in the tray was completely consumed and left only the burning woodpile (Fig. S4(a), S4(b)). The fire was used to test the water propelled rockets containing with MAP and MAP+Methyl Cellulose fire extinguishing agents. The performances of extinguishing agents were compared. The observed results were recorded as follows.

(1) Records of Radiant Heat Temperature using Thermal Camera:

- Pre-extinguishing temperature
- Post-extinguishing temperature (after the fire extinguishing agent was applied and the fire was completely suppressed).

(2) Time Measurement of Fire Burn and Extinguished: During the fire extinguishing worked, Records were done on the following information.

- Time at which fire suppression began.
- Time at which the fire was fully extinguished.

(3) The Observation of Fire Extinguishing Coverage

2.10 Statistical Analysis Used in the Experiment

Mean ($\bar{X}$), Standard Deviation (SD), T-test {Comparison between MAP and MAP+Methyl Cellulose (MC)}.

3. Results and discussion

3.1 The test of target accuracy by simulation program

When the initial pressure and initial water retaining ratio in the bottle were set at 4 bars with k_0 of 20%, 25%, 33%, 50%. The internal gas pressure was P_{in}. The jet velocity of water relative to the rocket was *ue*. The thrust force (F) generated by water discharge was calculated based on the water retaining ratio (k) through the numerical simulation. The resulting curves were presented as Fig. 3 (a, b, c, d) illustrating the variation of gas pressure inside the bottle and the variation of rocket's velocity. Also, explained the variation of thrust force as a function of the water retaining ratio. A flight model was developed to determine the ability of flame penetration to extinguish fire. The six-degree-of-freedom (6-DoF) dynamic model of the aerial system was derived based on a water-propelled system. The motion control system was designed using a Sliding-Mode Control (SMC) technique, comprising two control components: The first - Altitude and position control system; The second - Attitude control system where part of the desired attitude state was computed through the altitude and position controller.[41]

3.2 The Field-testing results of fire extinguishing rocket's detonation

The experiment using a dry chemical powder mixing with nano-cellulose ester was to establish the performance of firebreak and wildfire suppression in a field test area (Fig. S4(a) and S4(b)). The fire simulation demonstrated on wood-based sources included both the stacked woodpiles and wood log. The tests compared the performance of fire suppression of MAP and MAP+Methyl Cellulose (MC) as the extinguishing agents. This was to create a firebreak and a wildfire suppression in the firefighter's field test area. By using a long-range fire suppression approach with water propelled rocket, they were designed to deliver the fire extinguishing agent to the target area accurately. The MAP and MAP+Methyl Cellulose (MC) fire extinguishing agents were loaded into the nose cone of the rocket as shown in Fig. S1. The rockets were launched into a wooden fire source within 5 meters range to test Class A-fire suppression performance. Within 3 seconds, the results showed that the ignition reaction occurred in both MAP and MAP+Methyl Cellulose (MC) extinguishing agents, leading to the dispersal of the fire extinguishing agents across the burning source. The traditional wildfire extinguishing methods often encountered challenges in controlling wildfires. This study explored the new application of using cellulose ether-based fire extinguishing agents which transformed into a temperature-responsive hydrogel for wildfire suppression. When exposed to a high temperature, MAP+Cellulose Ether fire extinguishing agent changed its structure, forming a barrier-like protective layer essential for wildfire restraint. The

hydrogel created a dense carbon layer that acted as a strong firebreak, preventing wildfire spread. These temperature-reactive hydrogels were very interesting due to their unique thermal sensitivity which could be addressed the conventional hydrogels constraint. These various polymeric materials exhibited the rapid phase transitions upon the specific temperature threshold,[32,33] commonly referred to the lower critical solution temperature (LCST). In previous studies, the temperature-responsive hydrogels remained in a liquid state below the LCST and solidified into a gel when the temperature exceeded this threshold.[34,35] The thermal sensitivity of these hydrogels was attributed to the hydrophilic-hydrophobic component of their molecular structure. At room temperature, these hydrogels exhibited high fluidity and a low viscosity. At elevated temperatures, they, however, rapidly released water, and formed an adhesive coating on the surface of burning materials.[36]

Fig. 4 showed a visual of infrared camera that the wood burned quickly and fiercely. From the picture, it showed that the heat was truly high.

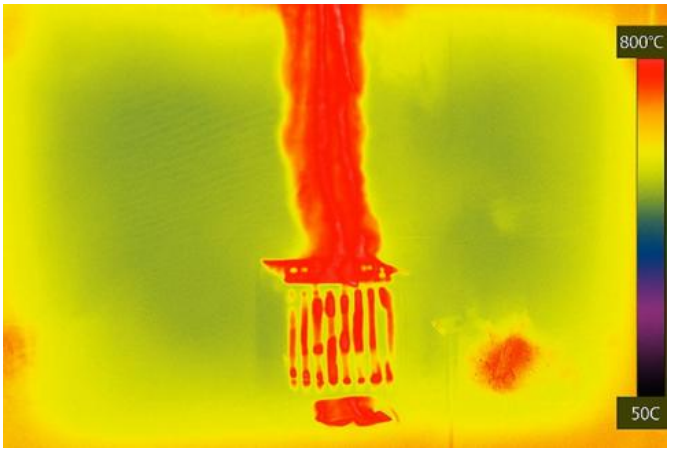

Fig. 4: Flames of heat generated from a burning wood pile.

The detonation reaction of the MAP+Methyl Cellulose (MC) fire extinguishing agent using the water propelled rocket to initiate a fire suppression reaction containing at the nose cone of the rocket was shown in Fig. S5(a). This reaction caused the extinguishing agent to disperse radially, covering the woodpile area. The agent then formed a gel layer on the wood surface, which reduced the temperature and cut down an oxygen supply as illustrated in Fig. S5(b). This process put a fire to extinguished, and it prevented from reignition within a short period as shown in Fig. S6(a). As a result, the MAP+Methyl Cellulose (MC) agent created a white gel layer coating on a wood surface. This formed gel reduced fuel evaporation, minimizing fire-induced damage to the wood. In contrast to the result of MAP as Fig. S6(b), there was an extensive black burn mark covering almost the entire wood surface.

Fig. 5(a) and 5(b) illustrated the fire suppression on the burning woodpile as captured by an infrared camera. It showed that when the burning wood pile reacted with the MAP+Methyl Cellulose (MC) fire extinguishing agent, it transformed into a gel to extinguish the fire. The thermal images depicted a gradual decrease in flame intensity until the fire was completely extinguished with no ignition recurring. Currently, temperature-responsive hydrogels have been being extensively studied in various fields, including medicine and agriculture.[37-39] For fire extinguishing applications, hydrogels should maintain a high viscosity and a strong adhesion at elevated temperatures, indicating that these hydrogels must exhibit a powerful thermal response in correlation with temperature changes. Most fire-extinguishing hydrogels were thermally stable, including isopropyl acrylamide and methyl cellulose derivatives.[40,41] Hydrogels containing Methyl Cellulose (MC) applied in various types of fire extinguishing began to rise viscosity when temperature increased. At 80°C, the material transformed nearly into a gel state. For example, the concentration of 5% or higher exhibited a viscosity exceeding 20 Pas. In previous studies, the solutions with concentrations of 2–8% were selected for a fire extinguishing test. For solutions with 2% and 4% concentration by weight, the fire extinguished times were 70 and 74 seconds, respectively. For solutions with 6% and 8% concentration by weight, the fire extinguished times were 60 and 115 seconds, respectively.[41]

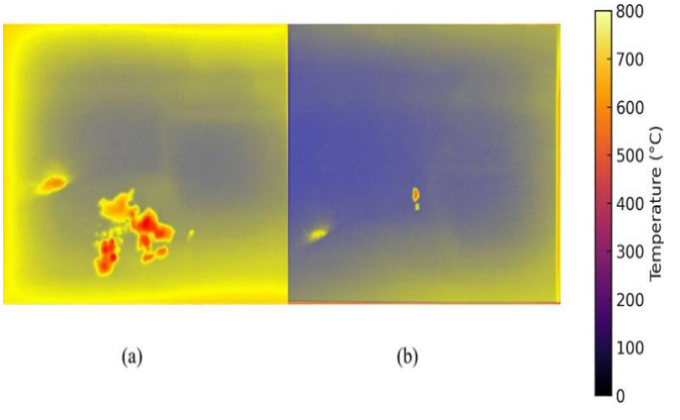

Fig. 5: The flame temperature as captured by an infrared camera began to decrease after the reaction of the MAP+Methyl Cellulose (MC) fire extinguishing agent; (a). The image of flame by an infrared camera showed that the flame was extinguished after the reaction of the MAP+Methyl Cellulose (MC) fire extinguishing agent; (b).

3.3 The Performance results of fire extinguishing agents

The Performances of fire extinguishing agents to Class A fire were evaluated as follows:

3.3.1 Radiant heat measurement

The thermal of radiant heat was measured by a thermal camera. The performances were done on Class A fire suppression by measuring 2 values per sample. One was done before applying to the fire extinguishing agent. The other was done after applying the fire extinguishing agent. The obtained data were presented as in Table 1. and Fig. 6.

Table 1: The data of thermal radiation temperature of Class A Fire before applying the fire extinguishing agent measured by thermal camera.

Test No.	Radiant heat temperature from burning source (℃)		Radiant heat temperature from burning source after applying the extinguishing agent (℃)	
	Fire Extinguishing Agent: MAP	Fire Extinguishing Agent: MAP+Methyl Cellulose (MC)	Fire Extinguishing Agent: MAP	Fire Extinguishing Agent: MAP+Methyl Cellulose (MC)
1.	546.04	437.4	308.14	121.43
2.	706.34	623.81	448.61	92.18
3.	673.27	679.22	293.54	73.45
$\bar{X} \pm SD$	641.88±84.63	580.14±126.68	350.09±85.62	95.68±24.18
P-Value	0.108 /0.01*			

Note: *There was a statistically significant difference (P ≤ 0.05).

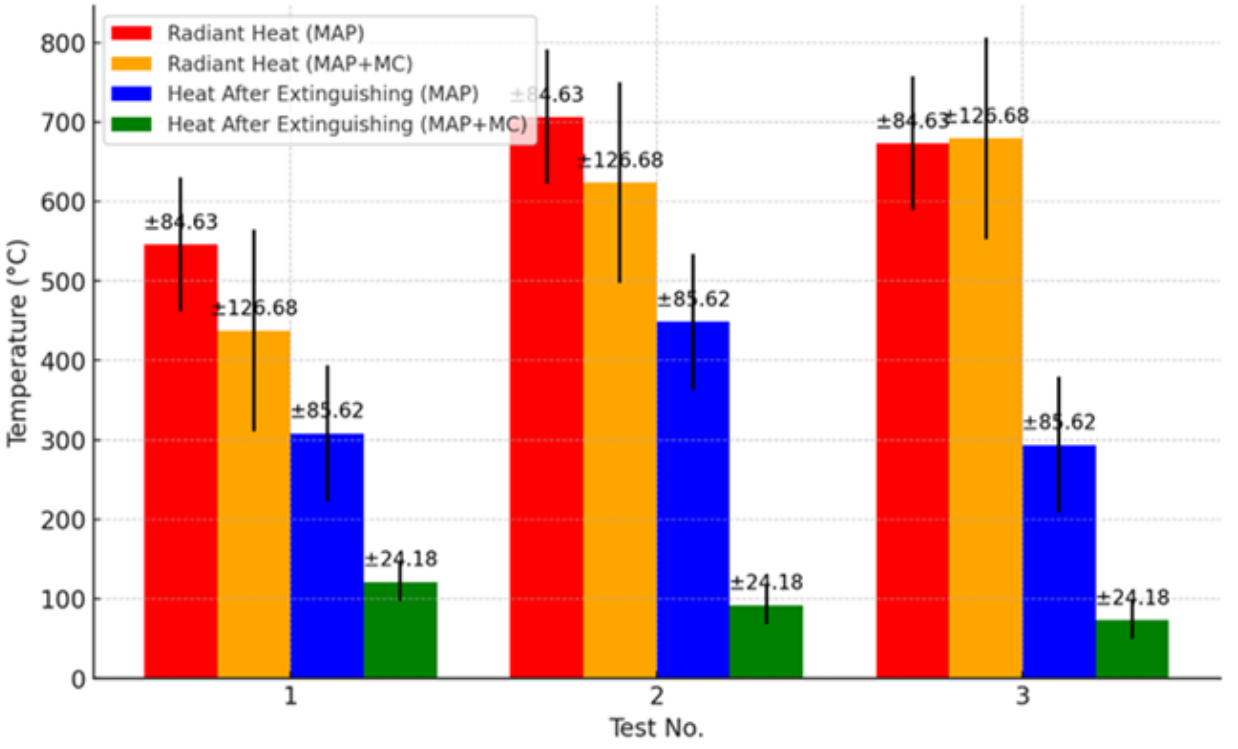

Fig. 6: Comparison of radiant heat and post-extinguishing temperatures with SD.

Table 2: Fire extinguished time of class A fire.

Test No.	Fire extinguished time (Seconds)	
	Fire Extinguishing Agent: MAP	Fire Extinguishing Agent: MAP+Methyl Cellulose (MC)
1.	9.30	5.11
2.	10.26	9.02
3.	12.68	6.93
$\bar{X}$±SD	10.74±1.74	7.02±1.95
P-Value	0.05*	

Note: *There was a statistically significant difference (P <= 0.05).

From Table 1 and Fig. 6, the analysis of the radiant heat temperature of the experimental woodpile before applying the fire extinguishing agent – MAP compared to MAP+Methyl Cellulose (MC), showed that the mean radiant heat temperatures of both fire extinguishing agents did not exhibit a statistically significant difference based on T-Test analysis. However, the radiant heat temperature of the experimental woodpile after applying the fire extinguishing agent - MAP compared to MAP+Methyl Cellulose (MC), revealed a statistically significant difference at the 0.05 level. The mean temperature after applying MAP was 350.09 ± 85.62°C, whereas the mean temperature after applying MAP+Methyl Cellulose (MC) was 95.68 ± 24.18°C.

3.3.2 The performance of fire suppression

(1) Fire Extinguished Time: The fire extinguished time of dry chemical agents for Class A fire was evaluated by time recording from the moment the extinguishing agent applied until the fire completely extinguished. A comparative time analysis was conducted between MAP and MAP+Methyl Cellulose (MC), with three repeat tests. The results were presented in Table 2.

From Table 2, the results compared the fire extinguished times of the fire extinguishing agents - MAP and MAP+Methyl Cellulose (MC). The mean fire extinguished times were analyzed using a T-test, revealing a statistically significant difference ($P > 0.05$). The mean fire extinguished time for MAP was 10.74 ± 1.74 seconds, whereas the mean fire extinguished time for MAP+Methyl Cellulose (MC) was 7.02 ± 1.95 seconds.

(2) Fire Extinguished Characteristics: The fire extinguished characteristics over the burning source were observed and recorded in Table 3. The assessment focused on the coating pattern over the burning source.

Table 3: Fire Extinguished Characteristics.

Test No.	Fire Extinguishing Agents	
	MAP	MAP+Cellulose Ether
1.	A thin layer of powder covering the wood surface	The gel well coating to the wood surface
2.	A thin layer of powder covering the wood surface	The gel well coating to the wood surface
3.	A thin layer of powder covering the wood surface	The gel well coating to the wood surface

Table 3, the performance of the fire suppression of dry chemical agents for Class A fire was revealed. MAP fire extinguishing agent formed a thin layer of dry chemical powder on each layer of wood surface with a large amount residue at the bottom. In contrast, the nano-cellulose ether-based fire extinguishing agent, MAP+Methyl Cellulose (MC) agent formed a gel coating as paste like texture on the wood surface distributed uniformly across the woodpile. This gel coating effectively reduced the temperature and cut off oxygen supply, thereby disrupting the fire triangle effectively. Additionally, the study of a water-based hydrogel fire extinguishing agent with low spraying, adhesion and spreading efficiency and fire extinguishing efficiency was studied. Inspired by the porous insulation material, a novel silica hydrogel fire extinguishing agent (SiKP) was successfully prepared by using micro-crosslinked silica aerogel and introducing phosphorus and potassium as fire extinguishing elements. SiKP showed excellent high-temperature adhesion properties on the wood surface, and its pH value met the application requirements. After spraying SiKP, the raging flame of the wood pile was extinguished rapidly within 2 seconds, and the burning time of the wood pile was reduced by 29.71%.[42] This is different from the current fire extinguishing agent used for wildfire suppression using Phos-Chek, which influences the species composition, survival and growth of vegetation in the grasslands of eastern Australia, in the Victoria Valley in the Grampian Mountains and Marlo in Eastern Gippsland. Both areas have long grassland vegetation. A single application of increasing concentrations of retardant (0.5, 1.0 and 1.5 L/m^2) resulted in complete necrosis of the primary vegetation and shoots of Allocasuarina paludosa, Banksia marginata, Leptospermum continentale and L. myrsinoides, and had an impact on other vegetation types.[43] In addition, Phos-Chek has been shown to influence the diversity and relative abundance of native and exotic species in serpentine soils, where a serpentine forest burned in 2017, affecting the plant diversity and abundance in the area.[44] It has also affected salmonids in local waters, with reduced salmon survival because of Phos-Chek exposure leading to a decline in salmonid populations.[45] In addition, Dali et al. studied the extinguishing time of liquid hydrocarbons using a carbon nanostructured suspension (CNS), a primarily cooling and diluting agent. Droplets of the suspension enter the combustion zone.[46] Which causes high heat to the boiling point. This process causes the combustion area to evaporate and cool down, and the flame will be extinguished by enough water vapor in the combustion area.[46-48] However, too high concentration of nanoparticles may cause the nanoparticles to aggregate, which will reduce the efficiency of heat conduction of the suspension and the specific heat of evaporation. From all the information, the use of cellulose ether hydrogel fire extinguishers has important advantages that are different from other fire extinguishers in terms of fire extinguishing efficiency that can reduce the temperature, can adhere to the wood well, cut off oxygen and is environmentally friendly in the area where this fire extinguisher is used, including being able to extinguish fires from a distance that is safe from using a water bottle rocket to the target area to extinguish.

4. Conclusion

The Field Performance Tests of Fire Suppression were

conducted by developing a fire extinguishing model to evaluate the performance of fire extinguishing on Class A fire. The study compared the performance of Mono Ammonium Phosphate (MAP), commonly known as ABC fire extinguishing agent, with Nano-Cellulose Ether combined with MAP. The results of the radiant heat temperature measured on Class A fire (wood-based materials) demonstrated that both extinguishing agents reduced the radiant heat emissions with no statistically significant difference. These were similar findings observed for Class B fire. When applying Mono Ammonium Phosphate (MAP), the mean radiant heat temperature was 350.09 ± 85.62°C. For Nano-Cellulose Ether combined with MAP (MAP+Cellulose Ether), the mean radiant heat temperature was 95.68 ± 24.18°C. For the performance of fire extinguished times between the two extinguishing agents, they were statistically different: The mean extinguished time for Mono Ammonium Phosphate (MAP) was 10.74 ± 1.74 seconds. And the mean extinguished time for MAP+Cellulose Ether was 7.02 ± 1.95 seconds. Additionally, the MAP fire extinguishing agent formed a thin powder layer over the wood surface, whereas the MAP+Cellulose Ether exhibited a gel-like coating effectively on the wood surface.

Acknowledgments

The authors are grateful to Suan Dusit University and Science Promotion Fund Research and Innovation Fund for funding this study.

Conflict of Interest

There is no conflict of interest.

Supporting Information

Applicable.

CRediT Statement

Nuttabodee Viriyawattana: Writing - Review and editing, Supervision, Project administration, Methodology, Funding acquisition, Conceptualization. **Surachat Sinworn:** Writing - Review & editing, Original draft, Visualization, Methodology, Data curation.

References

[1] I. M. Bartenev, S. V. Malyukov, M. A. Gnusov, D. S. Stupnikov, Study of efficiency of soilthrower and firebreak majer on the basis of mathematic simulation, *International Journal of Mechanical Engineering and Technology*, 2018, **9**(4), 1008-1018, doi: iaeme.com/ Home/journal/IJMET.

[2] D. Kasymov, V. Zima, V. Fateyev, Methods and devices used in the wildfire localization for the protection of forest ecosystems, *23rd International Symposium on Atmospheric and Ocean Optics: Atmospheric Physics*, Irkutsk, Russian Federation, July 3-7, 2017, 175, doi: 10.1117/12.2287438.

[3] W. E. Mell, S. L. Manzello, A. Maranghides, D. Butry, R. G. Rehm, The wildland–urban interface fire problem–current approaches and research needs, *International Journal of Wildland Fire*, 2010, **19**, 238-251, doi: 10.1071/wf07131.

[4] C. Warneke, J. P. Schwarz, J. Dibb, O. Kalashnikova, G. Frost, J. Al-Saad, S. S. Brown, W. A. Brewer, A. Soja, F. C. Seidel, R. A. Washenfelder, E. B. Wiggins, R. H. Moore, B. E. Anderson, C. Jordan, T. I. Yacovitch, S. C. Herndon, S. Liu, T. Kuwayama, D. Jaffe, N. Johnston, V. Selimovic, R. Yokelson, D. M. Giles, B. N. Holben, P. Goloub, I. Popovici, M. Trainer, A. Kumar, R. B. Pierce, D. Fahey, J. Roberts, E. M. Gargulinski, D. A. Peterson, X. Ye, L. H. Thapa, P. E. Saide, C. H. Fite, C. D. Holmes, S. Wang, M. M. Coggon, Z. C. J. Decker, C. E. Stockwell, L. Xu, G. Gkatzelis, K. Aikin, B. Lefer, J. Kaspari, D. Griffin, L. Zeng, R. Weber, M. Hastings, J. Chai, G. M. Wolfe, T. F. Hanisco, J. Liao, P. Campuzano Jost, H. Guo, J. L. Jimenez, J. Crawford, T. F. S. Team, Fire influence on regional to global environments and air quality (FIREX-AQ), *Journal of Geophysical Research: Atmospheres*, 2023, **128**, e2022JD037758, doi: 10.1029/2022jd037758.

[5] M. W. Jones, J. T. Abatzoglou, S. Veraverbeke, N. Andela, G. Lasslop, M. Forkel, A. J. P. Smith, C. Burton, R. A. Betts, G. R. van der Werf, S. Sitch, J. G. Canadell, C. Santín, C. Kolden, S. H. Doerr, C. Le Quéré, Global and regional trends and drivers of fire under climate change, *Reviews of Geophysics*, 2022, **60**, e2020RG000726, doi: 10.1029/2020RG000726.

[6] I. Zacharakis, V. A. Tsihrintzis, Environmental forest fire danger rating systems and indices around the globe: a review, *Land*, 2023, **12**, 194, doi: 10.3390/land12010194.

[7] A. A. Loschilov, Simplified mathematical model of inhibition of exothermic process in modeling the extinguishing of a forest fire, *Fluid Dynamics*, 2023, **58**, 773-778, doi: 10.1134/s0015462823601043.

[8] N. Viriyawattana, S. Sinworn, Performance improvement of the dry chemical-based fire extinguishers using nanocalcium silicate synthesised from biowaste, *Journal of Fire Sciences*, 2023, **41**, 73-88, doi: 10.1177/07349041231168553.

[9] M. Arvidson, P. Mindykowski, Fire testing of alternative fixed fire-extinguishing systems for ro-ro spaces onboard ships, *Ships and Offshore Structures*, 2023, **18**, 423-428, doi: 10.1080/17445302.2022.2061768.

[10] Y. Zhang, B. M. Wu, Current advances in stimuli-responsive hydrogels as smart drug delivery carriers, *Gels*, 2023, **9**, 838, doi: 10.3390/gels9100838.

[11] Z. Huang, L. Yan, Y. Zhang, Y. Gao, X. Liu, Y. Liu, Z. Li, Research on a new composite hydrogel inhibitor of tea polyphenols modified with polypropylene and mixed with halloysite nanotubes, *Fuel*, 2019, **253**, 527-539, doi: 10.1016/j.fuel.2019.03.152.

[12] C. Zhou, Y. Tang, A novel sodium carboxymethyl ellulose/aluminium citrate gel for extinguishing spontaneous fire in coal mines, *Fire and Materials*, 2018, **42**, 760-769, doi: 10.1002/fam.2631.

[13] C. Wang, H. Shi, X. Wang, L. Song, Y. Hu, Carrageenan-vermiculite-dimethyl methyl phosphate ternary hybrid hydrogels for firefighting, *Fire and Materials*, 2023, **47**, 400-410, doi:

10.1002/fam.3105.
[14] H. Yılmaz-Atay, J. L. Wilk-Jakubowski, A review of environmentally friendly approaches in fire extinguishing: from chemical sciences to innovations in electrical engineering, *Polymers*, 2022, **14**, 1224, doi: 10.3390/polym14061224.
[15] C. Huang, Z. Dai, Z. Jiang, Y. Chen, M. Zhong, Wood stack fire tests to evaluate the influence of extinguishing medium and driving pressure on fire extinguishing efficacy of forest trees, *Thermal Science and Engineering Progress*, 2024, **49**, 102464, doi: 10.1016/j.tsep.2024.102464.
[16] S. Kaulfuß, F. Hofmann, Types and Strategies of Forest Fire Fighting, Freiburg, Germany, waldwissen.net, 2011, 1-4, www.waldwissen.net,12.09.
[17] F. R. Tangherlini, A new method of fighting wildfires, *Open Journal of Safety Science and Technology*, 2021, **11**, 27-33, doi: 10.4236/ojsst.2021.112003.
[18] Godoy, K, Data Journalism Meets Information Design: Creating A Complex Infographic About The Yarnell Hill Wildfire (Doctoral dissertation), University of New York, 2015, 1-44.
[19] K. Dickman, On the Burning Edge: A Fateful Fire and the Men Who Fought It, *A Fateful Fire and the Men Who Fought It*, Ballentine Books, New York, 2015, ISBN-0553392123.
[20] H. Li, Z. Du, Study on the development of aerial fire extinguishing munition for forest fires and fire extinguishing tests, *Case Studies in Thermal Engineering*, 2024, **55**, 104138, doi: 10.1016/j.csite.2024.104138.
[21] F. Zapata, Maneuvering and Stability Control System for Jet Pack, United States, 2014, US Patent, 2014/0103165.
[22] R. Li, Personal Propulsion Device, United States, 2007, US Patent 7,900,867.
[23] X. Liu, H. Zhou, Unmanned water-powered aerial vehicles: theory and experiments, *IEEE Access*, 2019, **7**, 15349-15356.
[24] J.E. Naidoo, Modelling, Design and Analysis of a Water Jetpack Powered by an Autonomous Underwater Vehicle (AUV) System, Master's Thesis, Pietermaritzburg, South African, University of KwaZulu-Natal, 2017, 240.
[25] H. Ando, Y. Ambe, A. Ishii, M. Konyo, K. Tadakuma, S. Maruyama, S. Tadokoro, Aerial hose type robot by water jet for fire fighting, *IEEE Robotics and Automation Letters*, 2018, **3**, 1128-1135, doi: 10.1109/LRA.2018.2792701.
[26] D.-H. Lee, T. Huynh, Y.-B. Kim, C. Soumayya, Motion control system design for a flying-type firefighting system with water jet actuators, *Actuators*, 2021, **10**, 275, doi: 10.3390/act10100275.
[27] C.-H. Tai, J.-T. Teng, S.-W. Lo, D.-S. Cheng, C. Wu, Numerical study with the interactions of blast waves in ambient area, *38th Fluid Dynamics Conference and Exhibit*, Seattle, Washington, AIAA, 2008, AIAA2008-3850, doi: 10.2514/6.2008-3850.
[28] L. Zheng, W. Quan, Experimental study of explosive water mist extinguishing fire, *Procedia Engineering*, 2011, **11**, 258-267, doi: 10.1016/j.proeng.2011.04.655.
[29] B.C. Fan, Q. Gang, G. Dong, J.F. Ye, The Time Evolution of Shock-Flame Interaction, *Explosion and Shock Waves*, 2003, **23**(6), 488-492.
[30] S. Adrey, S. Galyna, Firefighting method using automated system on the basis of Multiple Launch Rocket System, *7th International Conference Space Technologies: Present and Future*, Dnipro, 2019, 273.
[31] G. Solomon, Analytical calculation on rocket stability, *International Journal of Aeronautical Science & Aerospace Research*, 2020, **7**(3), 244-248, doi: 10.19070/2470-4415-2000030.
[32] Y. Yang, L. Liu, M. Chen, Study on thrust performance of small water rocket launch, *Journal of Physics: Conference Series*, 2022, **2313**, 012021, doi: 10.1088/1742-6596/2313/1/012021.
[33] E. Ruel-Gariépy, J.-C. Leroux, In situ-forming hydrogels: review of temperature-sensitive systems, *European Journal of Pharmaceutics and Biopharmaceutics*, 2004, **58**, 409-426, doi: 10.1016/j.ejpb.2004.03.019.
[34] S. C. Barros, A. A. da Silva, D. B. Costa, I. Cesarino, C. M. Costa, S. Lanceros-Méndez, A. Pawlicka, M. M. Silva, Thermo-sensitive chitosan–cellulose derivative hydrogels: swelling behaviour and morphologic studies, *Cellulose*, 2014, **21**, 4531-4544, doi: 10.1007/s10570-014-0442-9.
[35] L. Klouda, Thermoresponsive hydrogels in biomedical applications, *European Journal of Pharmaceutics and Biopharmaceutics*, 2015, **97**, 338-349, doi: 10.1016/j.ejpb.2015.05.017.
[36] M. Dai, Y. Shang, M. Li, B. Ju, Y. Liu, Y. Tian, Synthesis and characterization of starch ether/alginate hydrogels with reversible and tunable thermoresponsive properties, *Materials Research Express*, 2020, **7**, 085701, doi: 10.1088/2053-1591/abae28.
[37] W. Ch eng, X. Hu, J. Xie, Y. Zhao, An intelligent gel designed to control the spontaneous combustion of coal: Fire prevention and extinguishing properties, *Fuel*, 2017, **210**, 826-835, doi: 10.1016/j.fuel.2017.09.007.
[38] J. W. Lim, H.-J. Kim, Y. Kim, S. G. Shin, S. Cho, W. G. Jung, J. H. Jeong, An active and soft hydrogel actuator to stimulate live cell clusters by self-folding, *Polymers*, 2020, **12**, 583, doi: 10.3390/polym12030583.
[39] P. Jiang, Y. Cheng, S. Yu, J. Lu, H. Wang, Study on the effect of 1-butanol soluble lignin on temperature-sensitive gel, *Polymers*, 2018, **10**, 1109, doi: 10.3390/polym10101109.
[40] S. Chatterjee, P. C. Hui, C.-W. Kan, Thermoresponsive hydrogels and their biomedical applications: special insight into their applications in textile based transdermal therapy, *Polymers*, 2018, **10**, 480, doi: 10.3390/polym10050480.
[41] X. Hu, W. Cheng, W. Nie, Z. Shao, Synthesis and characterization of a temperature-sensitive hydrogel based on sodium alginate and N-isopropylacrylamide, *Polymers for Advanced Technologies*, 2015, **26**, 1340-1345, doi: 10.1002/pat.3682.
[42] L. Ma, X. Huang, Y. Sheng, X. Liu, G. Wei, Experimental study on thermosensitive hydrogel used to extinguish class a fire, *Polymers*, 2021, **13**, 367, doi: 10.3390/polym13030367.
[43] M. Xu, Y. Wei, A. Qin, Y. Xu, M. Xu, B. Li, L. Liu, Novel

silica hydrogel-based forest fire extinguishing agent: Construction, fire extinguishing performance and mechanism study, *Journal of Cleaner Production*, 2025, **486**, 144490, doi: 10.1016/j.jclepro.2024.144490.
[44] T. Bell, K. Tolhurst, M. Wouters, Effects of the fire retardant Phos-Chek on vegetation in eastern Australian heathlands, *International Journal of Wildland Fire*, 2005, **14**, 199-211, doi: 10.1071/wf04024.
[45] Z. Raposo, The influence of fire and fire retardant (Phos-chek®) on plant diversity and non-native species abundance in California's serpentine chaparral, *International Conference on Serpentine Ecology*, 2023, doi: 10.13140/RG.2.2.28226.35521.
[46] J. P. Dietrich, M. S. Myers, S. A. Strickland, A. Van Gaest, M. R. Arkoosh, Toxicity of forest fire retardant chemicals to stream-type chinook salmon undergoing parr–smolt transformation, *Environmental Toxicology and Chemistry*, 2013, **32**(1), 236-247, doi: 10.1002/etc.2052.
[47] F. A. Dali, G. L. Shidlovsky, M. S. Khasikhanov, R. U. Zalaev, P. R. Tagirova, S. S. Saidulaev, L. M. Masaeva, R. S. Erzhapova, The use of carbon nanotubes in the fire extinguishing of oil and oil products, *IOP Conference Series*: *Materials Science and Engineering*, 2020, **905**, 012011, doi: 10.1088/1757-899x/905/1/012011.
[48] D. Toropov, A. Ivanov, F. Dali, A. Perlin, A. Lebedev, G. Shidlovsky, Extinguishing characteristics of water suspensions with carbon nanostructures at extinguishing liquid hydrocarbons fires (oil and gas industry), *Delta*, 2019, **13**(1), 22-31, doi: 10.17423/delta.2019.13.1.55.